Charge Carrier Studies of Regioregular Polyalkylthiophene

Hiroshi Ito, Sota Ukai, Noritsugu Nomura, Kota Hayashi, Tadafumi Ozaki,
Yasuhito Muramatsu, Kazuhiro Marumoto and Shin-ichi Kuroda
Department of Applied Physics, Nagoya University, Nagoya 464-8603, Japan
Fax: 81-52-789-5164, e-mail: ito@nuap.nagoya-u.ac.jp

Charge carrier injection and conduction characteristics of regioregular poly(3-alkylthiophene)s are investigated by field-effect transistor (FET), electron spin resonance (ESR), and photoconductivity measurements. An FET using Al_2O_3 gate insulator is fabricated with solution-cast poly(3-hexylthiophene). FET hole mobility as high as 8.3×10^{-3} cm^2/(Vs) at room temperature is obtained at induced surface carrier density as high as 3.2×10^{13}cm^{-2}. At 80 K the mobility decreased by two orders of magnitudes with thermally activated temperature dependence. Induced carriers by applying voltages across a metal-insulator-semiconductor diode with poly(3-octylthiophene) are observed by ESR. At negative bias the ESR intensity increases and at positive bias the ESR intensity decreases, in accordance with the accumulation and depletion of positive polarons. Photoconduction of an Al-poly(3-octylthiophene)-ITO Schottky photocell at room temperature appears only for negative bias with slow response, indicating hole transport behavior. By mixing of 10 mol% fullerenes into the polymer, photoconduction under illumination of photon energy below 2 eV is largely enhanced with rapid response at both bias polarities, whereas photoconduction above 2 eV appears only in the case of negative bias. This indicates the improved electron mobility in the case of composites with fullerenes.

Key words: regioregular poly(3-alkylthiophene), field effect transistor (FET), Al_2O_3, electron spin resonance, metal-insulator-semiconductor (MIS) diode, photocurrent

1. INTRODUCTION

Conducting conjugated polymers attract considerable attention for application to active devices in plastic-based electronics such as field-effect transistors (FETs) [1,2] and photovoltaic cells [3]. Addition of long alkyl side chains to the main conjugated chain makes the conjugated polymers soluble in common solvents such as chloroform. Solubility enables low-energy and low-cost fabrication techniques of electronic devices taking full advantage of organic materials, such as ink-jet printing [4]. Among soluble polymers, regioregular poly(3-alkylthiophene) (RR-P3AT) is one of the most promising materials due to the reported high field-effect mobility of the order of μ=0.1 cm^2/Vs [5-8]. The direction of alkyl side chains in RR-P3AT is ordered regularly in what is called "heat-to-tail" arrangement [9]. Due to the self-packing of alkyl side chains, π stacking of thiophene rings on conjugated chains facilitates the formation of ordered microcrystalline domains with the lamella structure which enhances the carrier mobility [6,9-15].

In order to develop polymer devices into practical applications, improvements in efficiency and lifetime of the device are necessary. For this purpose, it is important to understand the underlying physics of charge carrier states and their transport in conjugated polymers. The charge carriers in non-degenerated conjugated polymers are understood in terms of nonlinear excitations such as polarons, bipolarons, appearing upon carrier injection or doping [16]. The conductive characteristics vary with the amount of injected or doped carriers, from the hopping transport of polarons in the low doping regime
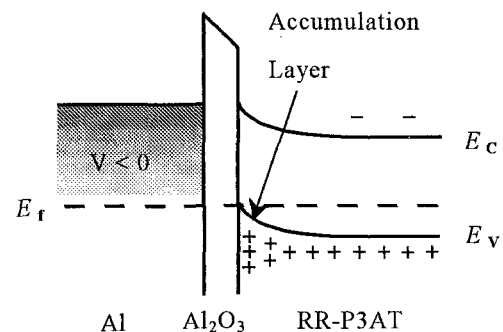

Fig. 1. Schematic energy diagram of the MIS structure. E_c, E_f, E_v are energies of conduction band edge, Fermi level, and valence band edge, respectively. Holes (+) are induced to the polymer by applying of a negative bias to Al electrode.

to the metallic conduction of delocalized states in the heavily doped regime [17]. The mechanism of evolution for the electronic state of the conjugated polymer is still obscure in spite of intensive studies for more than two decades. In the case of RR-P3AT, the spectroscopic signature of new type two-dimensional excitations possibly due to the increased interchain coupling is reported recently [12,18]. The nature of the charge carrier state of RR-P3AT is an intriguing problem for understanding the fundamental physics of conjugated polymers. Some experimental works have been carried out to study the evolution for the electronic state of RR-P3AT by the chemical doping techniques [19,20],

however, the chemical doping may affect the order of lamella structure in the microcrystalline regions in the RR-P3AT.

Recently, studies on electric field-induced charges in RR-P3AT have been performed spectroscopically [11,21,22]. A metal-insulator-Semiconductor (MIS) diode is formed with a polymer film as a semiconductor and a voltage is applied across the insulator layer. Then, field-induced charges are accumulated on the interface between the polymer film and the insulator layer as shown in Fig. 1. The evidences that induced charge carriers are of polaronic nature are found by electrically-induced new absorption lines [21] and changes in infrared-active vibration modes [22]. In order to study the transport of induced charge carriers, two more electrodes are added on the interface. The resulting structure is that of the FET. Study on charge carrier states induced by the field effect does not require any chemical dopant which disturbs the polymer structure. Moreover the charge concentration can be controlled easily by adjusting the gate voltage. In this paper we report the temperature-dependent I-V characteristics of regioregular poly(3-hexylthiophene) (RR-P3HT) FET and the observation of field-induced charge carriers by ESR on regioregular poly(3-octylthiophene) (RR-P3OT) MIS diode. In order to accumulate charge carriers to the higher extent compared to the conventional FETs using SiO_2 as a gate insulator [5-8,23], we used a highly capacitive Al_2O_3 as gate insulators.

Photoinjection is the other clean method to study the charge carrier state in conjugated polymers. Vigorous studies of photoinduced species by photo-induced absorption and light-induced ESR have been carried out [24,25]. Meanwhile, an enhancement of the photogeneration yield of charge carriers by mixing fullerene into the conjugated polymers attracts much attention as a novel method to study photocarriers [26,27]. The enhancement of ESR signals under illumination of photon energy of 1.9 eV in the regioregular poly(3-octylthiophene)-fullerene composite is observed [28]. In order to understand the conduction of photoinjected charge carriers in more detail, we studied the photocurrent of a Schottky diode photocell made of RR-P3OT and its composite with 10mol% fullerene, in view of the polarity of the photoinduced charge carriers in the composite system.

2. EXPERIMENTAL
2.1 Fabrication of FETs and MIS diodes and conductive and ESR measurements

In Figs. 2(a) and 2(b), we show schematic structures of the FET and MIS devices used for conductive and ESR measurements. The fabrication procedure is almost the same, except the selection of substrates and Au electrode preparation. For the FET, a 10×14 mm glass substrate (Matsunami Co. white-cut glass) was used. For the MIS, a 3×20mm quartz substrate (Eikosha Co.) was used in order to insert the device into the ESR quartz sample tube of inner diameter of 3.1 mm. Quartz substrate is suitable for ESR measurements since it produces no ESR signal. Both substrates were sonicated in ethanol and heat-treated close to the melting point in order to remove moisture, and again sonicated

in ethanol. Then the substrate was set in a vacuum evaporation system (ULVAC VPC-250K1) equipped with rf-sputtering gun (AJA ST-20) under dry N_2 gas atmosphere.

Al was evaporated onto the substrate as a gate electrode. Bonding between Al and Al_2O_3 is strong enough to avoid damages during the Al_2O_3 sputtering process. The thickness was about 100 nm. Then an Al_2O_3 gate insulator layer was deposited by rf-sputtering onto the Al gate electrode under a low pressure Ar gas flow. The sputtering condition was experimentally determined in order to maximize the product of the specific dielectric constant and the breakdown voltage, which is proportional to the induced charge carrier density. The best condition was that the power was 200-300 W and the Ar pressure was 10-20 mTorr. The substrate should be located not at the center of plasma but at the edge of plasma in order to have good results. The temperature of the substrate was not controlled, but the substrate was heated up to about 100°C during the sputtering. The deposition rate was 3.5nm/min. The thickness of the Al_2O_3 layer was 200 ± 40 nm. The capacitance per unit area C_i was ~30 nF/cm^2. The breakdown voltage was 10 MV/cm. The present Al_2O_3 film has lower capacitance but higher breakdown voltage than that of the recent work [29]. The specific dielectric constant ε was about 7. The leak current before the breakdown was the order of nA. The capacitance of the Al_2O_3 gate insulator was hardly changed between 80 and 296 K. Fig. 3 shows an AFM image (1μm×1μm) of the rf-sputtered Al_2O_3 on the Al gate electrode. The surface is rough due to the large grain size (100-200 nm). Small grain size was obtained by reducing the power to 50 W, however it took long time (more than 12 hours) to deposit the film. The specific dielectric constant of the Al_2O_3 at this power
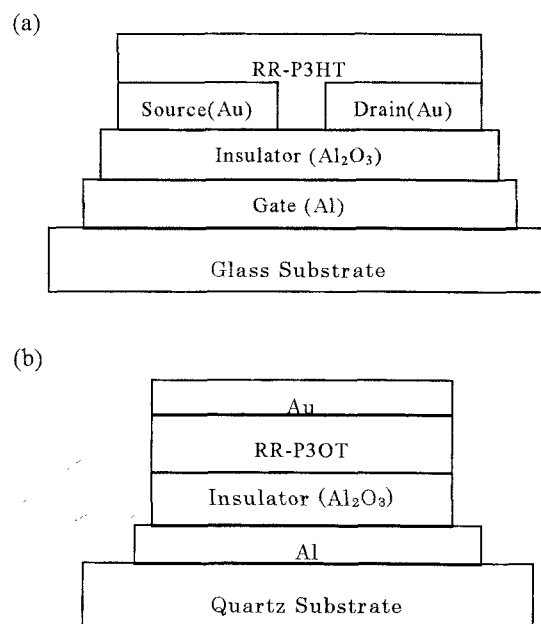
(a)

(b)

Fig. 2.   Schematic structure of the FET (a) and the MIS diode for ESR measurements (b), using Al_2O_3 as insulators to inject carriers into RR-P3AT.
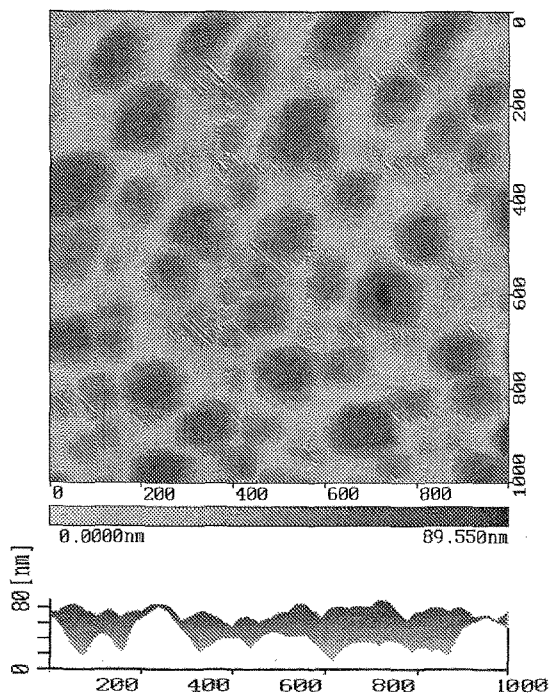
Fig. 3. An AFM image (1 μm × 1 μm) and the cross-sectional profile of the sputtered Al_2O_3 film on the Al electrode. The white portion in the cross-sectional profile is the cross section at 1000 nm on the vertical axis of the surface image. The tone of the dark portion represents the variation of the cross section at each vertical position from 1000 to 0 nm.

reduced to less than 4, possibly due to the contaminants during the long sputtering time such as pump oil vapor.

In the case of the FET, Au was evaporated though a shadow mask with thickness of 50 nm onto the Al_2O_3 gate insulator as the source and drain channel electrodes. The channel electrodes were straight, not interdigitated. We used Au to form ohmic contacts to RR-P3AT. The distance between the electrodes, that is, the channel length L was 50μm and the channel width W was 4mm. In the case of the MIS, an Au electrode was evaporated as the final step after casting the RR-P3OT film on the Al_2O_3 surface.

Regioregular-poly(3-hexylthiophene) (RR-P3HT) and regioregular-poly(3-octylthiophene) (RR-P3OT) (head-to-tail ratio 98.5%) [9] were purchased with Aldrich, Co. Ltd. For the FET, RR-P3HT was used because of the highest reported mobility value among commercially available RR-P3ATs [8]. For the ESR measurements, RR-P3OT was used. The material was soaked into a NH_3 water solution and a CH_3OH solution for more than 1 h to wash up and dedope it [5]. Dried RR-P3AT was dissolved in $CHCl_3$ solution until the saturated solution (about 0.20 wt%) at 296 K, under 1 atm NH_3 and N_2 gas atmosphere. Then the solution was drop-cast on the device. The thickness of RR-P3AT film was about 1μm. We used a drop-casting method to enhance the formation of the self-organized lamella structure [12]. The drop-casting was carried out under Ar gas with low concentration of NH_3 to reduce unintentionally doping by oxygen.

For the FET measurement, the drain current I_d was measured as a function of the drain voltage V_d at various gate voltages V_g applied between the gate and source electrodes. The source electrode was grounded. The I_d was measured with a Keithley 2000 digital multimeter as a voltage drop through a resistor (100 kΩ) connected in series, in order to avoid damages in case of a sudden breakdown of the gate insulator. In this paper, we call I-V characteristic for this type of measurement. The measurements were carried out in a temperature range from 80 to 296 K under low vacuum (about 0.1Pa) or low pressure N_2.

For ESR measurements, the MIS device was inserted into a quartz sample tube and evacuated down to 10^{-6} torr and sealed with 100 torr high purity He gas. The ESR spectra were measured with a Bruker EMX X-band spectrometer, under applied voltages supplied from Keithley 2400 source-measure unit.

2.2 Fabrication of photocell and photoconduction measurements

For photoconduction measurements, a glass with presputtered 2mm width ITO strips was used as substrate. Then the toluene solution of the RR-P3OT, or mixed solution of RR-P3OT with 10 mol% fullerene was drop cast onto the substrate. In the case of mixed solution with fullerene, the solution was sonicated for 1 h for better uniform mixing. The thickness of the cast film is 5 μm. Then the upper Al electrode was evaporated to form the rectifying contact.

The photocurrent was measured with an Agilent 4339B high resistance meter under the illumination of the monochromated light from a halogen lamp (500W). The power of irradiation onto the photocell was 0.01 to 0.1 mW/cm^2. The light was illuminated from the ITO side of the sample.

3. RESULTS

3.1 FET characteristics

Fig. 4 shows the I-V characteristics at 296 K (a) and at 80 K (b) in the accumulation mode of the FET. The gate voltage has to be negative in order to accumulate holes in the polymer. For the I-V characteristic at 296 K, FET is in the linear regime below V_d=-30 V and the pinch-off regime above V_d=-30 V, although I_d is not constant even in the pinch-off regime. This kind of the behavior is often observed for the conjugated polymers [1,5]. For the I-V characteristics at 80 K, it is difficult to distinguish from the linear and the pinch-off regimes. The mobility was evaluated at the pinch-off point using the following two equations [1,2,5,30],

$$I_d = \frac{C_i W}{L} \mu (V_g - V_t - \frac{1}{2} V_d) V_d, \quad V_d < V_g - V_t, \quad (1)$$

$$I_d = \frac{C_i W}{2L} \mu (V_g - V_t)^2, \quad V_d \geq V_g - V_t, \quad (2)$$

where μ is the mobility and V_t is the threshold voltage. The threshold voltage is evaluated by the linear extrapolation of the V_g dependence of $I_d^{1/2}$ down to I_d=0, as shown in Figs. 5(a) and 5(b). The threshold voltage is V_t=+18.6 V at 296 K and V_t=+17.9 V at 80 K respectively. At the pinch-off point where the equation
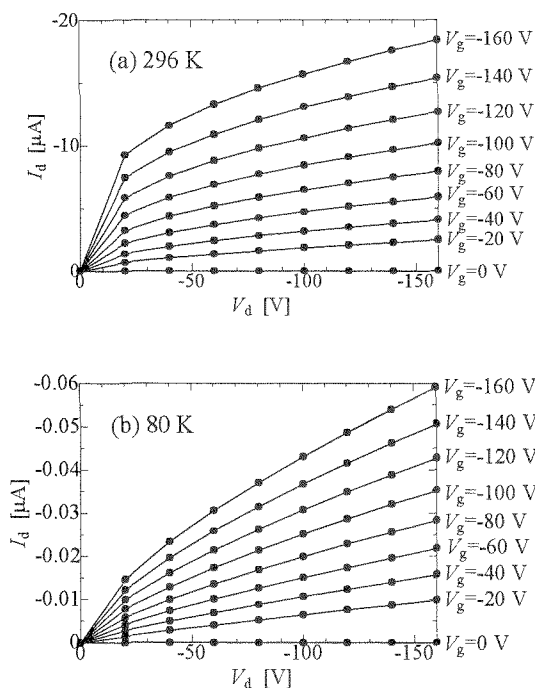
Fig. 4. I-V characteristics of RR-P3HT FET at (a) 296 K and (b) 80 K. Solid lines are visual guides.
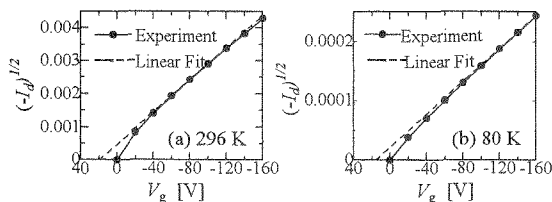

Fig. 5. $(-I_d)^{1/2}$ versus V_g curves for determining the threshold voltages at 296 K (a) and 80 K (b). Solid lines are visual guides and broken lines are linear extrapolations.

$V_d = V_g - V_t$ holds, eqs. (1) and (2) gives the same value of I_d. The mobility is evaluated by finding the point of $V_d = V_g - V_t$ on the I-V characteristic at each V_g. At 296 K, the mobility increases from 5.1×10^{-5} cm²/Vs to 8.3×10^{-3} cm²/Vs changing V_g from 0 V to -160 V. At 80K, the mobility increases from 2.1×10^{-7} cm2/Vs to 2.8×10^{-5} cm²/Vs in the same V_g range. The application of the V_g of -160 V brought about the rise in mobility by two orders of magnitude at each temperature. Fig. 6(a) shows the temperature dependences of the mobility at each V_g. By lowering the temperature from 296 to 80 K, the mobility decreased by two orders of magnitude. The decrease of the mobility is scaled by Arrhenius plot as shown in Fig. 5(b), indicating that RR-P3HT film shows a thermally activated conduction at each V_g.

3.2 ESR measurement of the MIS device

The intensity of an ESR signal at $g=2.003$ of linewidth ~3 G, coming from polarons in RR-P3OT, changed according to the application of volatges across the Al and Au electrodes of the MIS device. The ESR
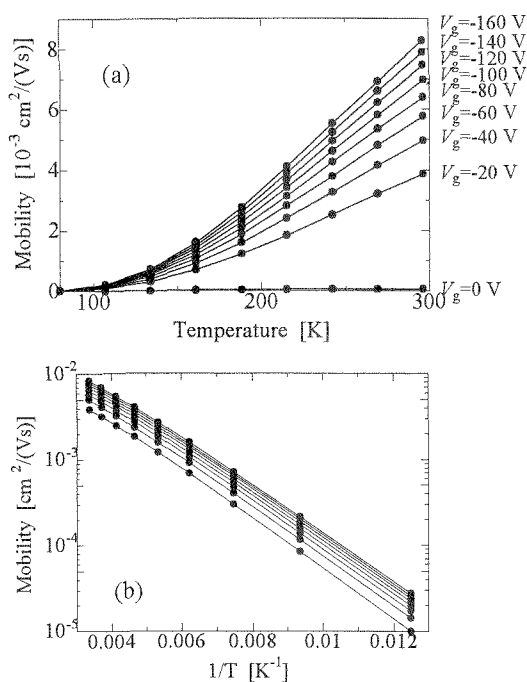

Fig. 6. Temperature dependence of the mobility at various gate voltages in linear plot (a) and in Arrhenius plot at gate voltages -20 to -160 V (b). Solid lines are visual guides.

intensity increased under negative bias applied to the Al electrode. Under positive bias to the Al electrode, the ESR intensity decreased. The increase and decrease of the intensity represent the accumulation and depletion of the holes at the interface between Al_2O_3 and RR-P3OT.

3.3 Photoconductivity measurement

The photocurrent of a Schottky diode photocell of RR-P3OT sandwiched with Al and ITO at room temperature appears only for positive bias applied to ITO with slow response at low irradiation power of 0.01-0.1 mW/cm² [31]. By mixing of 10 mol% fullerenes into RR-P3OT, photoconduction under illumination of photon energy below 2 eV is largely enhanced with rapid response [27] for both bias polarities. In Fig. 7, the bias dependence of the photocurrent under illumination at 640 nm (1.94 eV, intensity 0.05 mW/cm²) is shown with and without mixing fullerene into the RR-P3OT. On the other hand, the photocurrent appears only for positive bias under illumination of photon for energy above 2 eV, as shown in the action spectra (Fig. 8).

4. DISCUSSION

4.1 Mobility and induced charge carriers by field-effect

The observed value of the mobility at 296 K is less than those reported for FETs using SiO_2 as gate insulator (0.05-0.2 cm²/Vs [5-7]). This may be because the flatness of the Al_2O_3 surface is inferior to the flatness of SiO_2 surfaces as shown in Fig. 3. The flat surface facilitates the formation of the ordered lamella structured RR-P3HT with the large spatial correlation length [14].

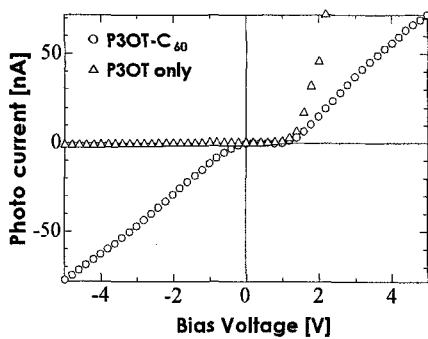The temperature dependence of the mobility fits well

Fig. 7. Photocurrent as a function of bias voltages for RR-P3OT and RR-P3OT-10% fullerene composite at 640 nm (1.94 eV) illumination.
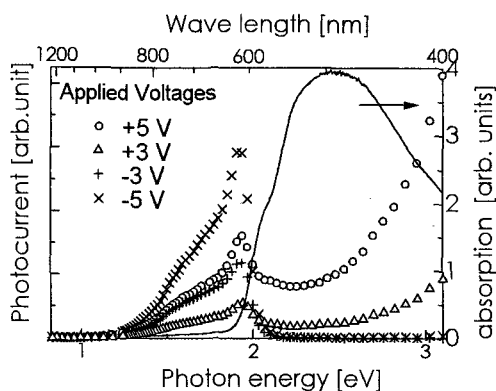

Fig. 8. Photocurrent action spectra at various bias voltages of RR-P3OT-10% fullerene composite. Note that the irradiation power is not constant but varies in the range of 0.01-0.1 mW/cm², according to the dispersion of the halogen lamp. Optical absorption spectrum is also indicated.

to Arrhenius plots at each V_g as shown in Fig. 5(b). This indicates that at least in the measured temperature range, the transport mechanism is via thermally activated hopping among the deep trapping sites. On the other hand, the variable range hopping model has been extensively used to explain the charge transport mechanism in many highly chemically-doped poly(3-alkylthiophene)s in which the high density of state grows in the band energy gap [19,32,33]. In the present study, the density of state may not be so high enough for the variable range hopping mechanism to work. Aleshin et al. reported the two-dimensional variable range hopping mobility in RR-P3HT by FET with SiO₂ as gate insulator [23]. This may be ascribed to the surface flatness of the SiO₂ in which deep trapping sites are scarce compared to the Al₂O₃. The Arrhenius plot of the mobility gives the activation energy E_A. The value of E_A is 55 meV, which is smaller compared to the former reports [6]. The activation energy decreased slightly with the increase of the gate voltage, but the decrement was not large as reported for FET with SiO₂ as gate insulator [6,30]

The carrier density per unit area $n_\square$ induced by the field-effect is given by,

$$n_\square = \frac{C_i |V_g - V_t|}{q}, \quad (3)$$

where q is the elementally charge. At 296 K, the maximum induced carrier density was 3.35×10^{13} cm⁻² at $V_g = -160$ V. The value hardly changed with the decrease of the temperature down to 80 K. Assuming that the ordered lamella structure of RR-P3HT is formed on the surface of the Al₂O₃ gate insulator [15], the doping level induced by the field effect is calculated. Since the unit cell of the lamella structure is 0.78 nm $\times$ 0.77 nm which consists of four thiophene rings [12,13], the area occupied by one thiophene ring is 1.5×10^{-15} cm². Then the doping level expressed per thiophene ring was about 4 % at $V_g = -160$ V, if all of the induced carriers are confined within one molecular layer of RR-P3HT at the interface. In the case of the electrochemical doping at room temperature, the mobility increases above the doping level of 1 % [34]. At the doping level of 4 % the mobility is about 2×10^{-2} cm²/Vs and is still on the way of rapid increase. The increase of the mobility is attributable to the formation of bipolaron states with shallower trapping, since the ESR signal increase is suppressed above the doping level of 1 % [20,34]. It is possible that induced charges in the present FET may form bipolaron states with reduced activation energy.

On the other hand, induced charge carriers by the field effect are observed by ESR measurements on the MIS device made with RR-P3OT and Al₂O₃ insulator, as an increase and a decrease of ESR intensity according to the polarity of applied voltages. It is found that the induced charge carriers have spins, so that the main field-induced species are polarons, not bipolarons. Detailed study of field-induced ESR signals will be presented elsewhere.

4.2 Photogenerated carriers in the Schottky photocell

In the Schottky photocell, the photogeneration of carriers mainly takes place at the interface of the rectifying electrode [35]. In the case of irradiation from ITO side, the light attenuates at the Al electrode where the charge is generated. The decrease of the photocurrent near 2.2-2.5 eV should be interpreted as such 'filter effect' [35]. Apart from the filter effect, photocurrent enhancement at 1.5-2.0 eV is understood as caused by the fullerene mixing effect. The range of the photon energy of the photocurrent enhancement is wider than the former photoconductivity report on regiorandom poly-3-alkylthiophenes [27]. The wide range of enhancement is observed also by the light-induced ESR measurements [28].

The photocurrent is observed for both polarity at the photo energy region of the photocurrent enhancement. The enhancement of the photocurrent for negative bias is also observed in the other composite system of MEH-PPV-CN-PPV heterojunctions in which CN-PPV is conductive for electrons [36]. The bipolar nature of the photocell indicates an increase in the electron mobility possibly due to the conduction of electrons on the fullerene molecules. It is possible that electrons hop along percolated fullerene paths in the case of negative bias. The role of the electron in the photoconductivity in the negative bias is demonstrated

by a slight change in photocurrent at 260 K, by the structural phase transition of fullerene [37].

5. CONCLUDING REMARKS

We studied the conductive characteristics of field-induced charge carriers of RR-P3HT by using the FET with Al_2O_3 as gate insulator. The maximum values of the mobility are 8.3×10^{-3} cm^2/Vs at induced surface carrier density of 3.35×10^{13} cm^{-2}, in the applied gate voltage of V_g=-160 V at 296 K. With the decrease of the temperature down to 80 K, the mobility decreased by two orders of magnitude with thermally activated temperature dependence. The transport mechanism of RR-P3HT film in this study occurs via thermally activated hopping among deep trapping sites.

The induced charge carriers at the interface of an MIS diode are observed by ESR measurements. It is found that induced charge carriers have spins and are polarons.

Photocurrent of a schottkey photocell of RR-P3OT-10% fullerene composites shows bipolar behavior below irradiation photo energy of 2 eV. This implies the increased electron transport in the composite. Measurements on FET made with polymer-fullerene composite is encouraged to study the conduction characteristics of charge carriers in the composite.

References

[1] G. Horowitz, *Adv. Mater.*, **10**, 365-377 (1998).

[2] C. D. Dimitrakopoulos and P. R. L. Malenfant, *Adv. Mater.*, **14**, 99-117 (2002).

[3] C. J. Brabec, N. S. Sariciftci and J. C. Hummelen, *Adv. Funct. Mater.*, **11**, 15-26 (2001).

[4] H. Sirringhaus, T. Kawase, R. H. Friend, T. Shimoda, M. Inbasekaran, W. Wu, and E. P. Woo, *Science*, **290**, 2123-2126 (2000).

[5] Z. Bao, A. Dodabalapur, and A. J. Lovinger, *Appl. Phys. Lett.*, **69**, 4108 -4110 (1996).

[6] H. Sirringhaus, N. Tessler, and R. H. Friend, *Science*, **280**, 1741-1744 (1998).

[7] G. Wang, J. Swensen, D. Moses, and A. J. Heeger, *J. Appl. Phys.*, **93**, 6137-6141 (2003).

[8] K. Kaneto, W. Y. Lim, W. Takashima, T. Endo and M. Rikukawa, *Jpn. J. Appl. Phys.*, **39**, L872-L874 (2000).

[9] T. A. Chen, X. Wu and R. D. Rieke, *J. Am. Chem. Soc.*, **117**, 233-244 (1995).

[10] T. Kawai, M. Nakazono and K. Yoshino, *J. Phys.: Cond. Mat.*, **6**, 4029-4036 (1994).

[11] T. Yamamoto, D. Komarudin, M. Arai, B.-L. Lee, H. Suganuma, N. Asakawa, Y. Inoue, K. Kubota, S. Sasaki, T. Fukuda, and H. Matsuda, *J. Am. Chem. Soc.*, **120**, 2047-2058 (1998).

[12] H. Sirringhaus, P. J. Brown, R. H. Friend, M. M. Nielsen, K. Bechgaard, B. W.W. Langeveld-Voss, A. J.

H. Spiering, R. A. J. Janssen, E. W. Meijer, P. Herwig, and D. M. de Leeuw, *Nature*, **401**, 685-688 (1999).

[13] A. J. Lovinger, Z. Bao, H. E. Katz, and A. Dodabalapur, *Polym. Mater. Sci. & Eng.*, **81**, 234-235 (1999).

[14] K. E. Aasmundveit, E. J. Samuelsen, M. Guldstein, C. Steinland, O. Flornes, C. Fagermo, T. M. Seeberg, L. A. A. Pettersson, O. Inganas, R. Feidenhans'l, and S. Ferrer, *Macromolecules*, **33**, 3120-3127 (2000).

[15] T. Yamamoto, H. Kokubo, T. Morikita, *J. Polym. Sci.:Part B: Polym. Phys.*, **39**, 1713-1718 (2001).

[16] S. Kuroda, K. Murata, Y. Shimoi, S. Abe, T. Noguchi, and T. Ohnishi, "Materials and Measurements in Molecular Electronics", Ed. by K. Kajimura and S. Kuroda, Springer Proceedings in Physics, Vol. 81, Springer-Verlag, Tokyo (1996) pp. 256-267.

[17] For example, A. J. Epstein, "Organic Electronic Materials", Ed. by R. Farchioni and G. Grosso, Springer Verlag, Berlin (2001) pp. 3-37.

[18] R. Osterbacka, C. P. An, X. M. Jiang, and Z.V. Vardeny, *Science*, **287**, 839-842 (2000).

[19] T. Yamamoto, M. Abla, T. Shimizu, D. Komarudin, B.-L. Lee, E. Kurokawa, *Polymer Bulletin*, **42**, 321-327 (1999).

[20] X. Jiang, Y. Harima, K. Yamashita, Y. Tada, J. Ohsita, and A. Kunai, *Chem. Phys. Lett.*, **364**, 616-620 (2002).

[21] P. J. Brown, H. Sirringhaus, M. Harrison, M. Shkunov, and R. H. Friend, *Phys. Rev. B*, **63**, 125204-1-11 (2001).

[22] Y. Furukawa, S. Furukawa, S. Maekawa, M. Ishima, *Macromol. Symp.*, **184**, 99-106 (2002).

[23] A. N. Aleshin, H. Sandberg, H. Stubb, *Synth. Met.*, **121**, 1449-1450 (2001).

[24] P. A. Lane, X. Wei, Z. V. Vardeny, *Phys. Rev. Lett.*, **77**, 1544-1547 (1996).

[25] S. Kuroda, K. Marumoto, H. Ito, N. C. Greenham, R. H. Friend, Y. Shimoi and S. Abe, *Chem. Phys. Lett.*, **325**, 183-188 (2000).

[26] N. S. Sariciftci, L. Smilowitz, A. J. Heeger and F. Wudl, *Science*, **258**, 1474-1476 (1992).

[27] K. Yoshino, X. H. Yin, S. Morita, T. Kawai and A. A. Zakhidov, *Solid State Commun.*, **85**, 85-88 (1993).

[28] K. Marumoto, N. Takeuchi, T. Ozaki and S. Kuroda, *Synth. Met.*, **129**, 239-247 (2002).

[29] W. H. Ha, M. H. Choo, and S. Im, *J. Non-Cryst. Solids*, **303**, 78-82 (2002).

[30] A. R. Brown, C. P. Jarret, D. M. de Leeuw, and M. Matters, *Synth. Met.*, **88**, 37-55 (1997).

[31] S. B. Lee, K. Yoshino, J. Y. Park and Y. W. Park, *Phys. Rev. B*, **61**, 2151-2158 (2000).

[32] I. Youm, M. Cadene, and D. Laplaze, *J. Mater. Sci. Lett.*, **14**, 1712-1714 (1995).

[33] R. Singh, A. Kaur, K. L. Yadav and D. Bhattacharya, *Curr. Appl. Phys.*, **3**, 235-238 (2003).

[34] Y. Kunugi, Y. Harima, K. Yamashita, N. Ohta and S. Ito, *J. Mater. Chem.*, **10**, 2673-2677 (2000).

[35] K. Kaneto, K. Takayama, W. Takashima, T. Endo and M. Rikukawa, *Jpn. J. Appl. Phys.*, **41**, 675-679 (2002).

[36] G. Yu and A. J. Heeger, *J. Appl. Phys.*, **78**, 4510-4515 (1995).

[37] I. Balberg, R. Naidis, M.-K. Lee, J. Shinar and L. F. Fonseca, *Appl. Phys. Lett.*, **79**, 197-199 (2001).